RADIOCHEMISTRY AND RADIOPHARMACEUTICALS

Sequential Imaging of Indium-111-Labeled Monoclonal Antibody in Human Mammary Tumors Hosted in Nude Mice

Ban An Khaw, H. William Strauss, Susan L. Cahill, Howard R. Soule, Thomas Edgington, and John Cooney

Massachusetts General Hospital, Boston, Massachusetts, Research Institute of Scripps Clinic, La Jolla, California, and Mallinckrodt Inc., St. Louis, Missouri

Using a bifunctional chelating agent, indium-111 was attached to a monoclonal antibody 10-3D2, specific for a 126-kilodalton phosphoglycoprotein antigen associated with human mammary carcinoma, and was then used to localize and visualize human mammary tumors hosted in nude mice. Simultaneous tumor concentration of In-111-10-3D2 was eight times greater than that of control I-125-MOPC-21. Uptake of $F(ab')_2$ and Fab of 10-3D2 was also compared. The scintigrams demonstrated that intact antibody provided the best images. Control In-111-labeled MOPC-21 and plasma did not show specific localization in the tumor. Uptake of In-111-labeled 10-3D2 was also compared in two lines of human mammary tumors, BT-20 and HS-578T. Imaging with 10-3D2 was better for BT-20 than for HS-578T. These studies demonstrated that (a) In-111-10-3D2 can be utilized to image human mammary tumors hosted in nude mice; (b) intact antibody provided the best tumor images, although $F(ab')_2$ had optimal target-to-background ratios for earlier imaging; and (c) different mammary tumor lines with possibly different concentrations of tumor-associated antigen showed different rates of uptake and apparent saturation with 10-3D2.

J Nucl Med 25: 592–603, 1984

Although the recognition of antibodies as potential target-specific immunologic agents dates back to the turn of this century (*1*), Pressman and Keighley in 1948 were the first to demonstrate conclusively the localization of radiolabeled antibodies in specific target organs in vivo (*2*). Since then, antibodies have been used for detection and visualization of various malignant tissues in experimental animals (*3–6*), and man (*7–10*). Early studies used the immune-globulin fractions of tumor-specific antisera for detection of tumors (*11,12*), or nonspecific markers such as antifibrinogen (*13*), usually labeled with iodine-131. The next generation of immunologic tumor-imaging agents, antibodies to oncofetal proteins (*9,14–16*), were also labeled with I-131. Advances in the production of tumor-specific or -associated antibodies, however, required the advent of monoclonal antibody technology (*17–19*) to provide a reliable source of large quantities of a specific antibody directed against a single epitope. Improvements in radiolabeling (*20–23*) now permit the formation of stable complexes of antibody with either technetium-99m or indium-111. These radiolabels allow high-quality images to be recorded with a low radiation burden.

Before selecting among the possible radiolabeled antibodies directed against specific single epitopes, one must establish which portion of the antibody molecule provides the best images in vivo. Recent studies suggest that $F(ab')_2$ may have superior imaging characteristics to Fab (*24*). To evaluate this point, studies were undertaken with an indium-111-labeled monoclonal antibody (10-3D2)—specific for a 126-kd phosphoglycoprotein (pgp) antigen associated with human mammary tumors (*25*)—in order to detect and visualize such tumors by gamma imaging in nude mice. In vivo uptake

Received Sept. 7, 1984; revision accepted Mar. 7, 1984.

For reprints contact: Ban An Khaw, PhD, Cellular and Molecular Research Lab, Jackson 13, Massachusetts General Hospital, Boston, MA 02114.

of whole antibody in the tumor was compared with uptakes of $F(ab')_2$ and Fab to determine their relative kinetics in the tumors. In addition, we compared the in vivo avidity of 10-3D2 for two human mammary-tumor lines (BT-20 and HS-578T).

MATERIALS AND METHODS

Production of monoclonal antibody 10-3D2. This was prepared by hybridization of immune spleen cells with SP2/O murine myeloma cells, as described by Soule et al. (*25*). Briefly, a human mammary-tumor cell line (BT-20) was used to immunize female BALB/c mice by peritoneal injections. Booster i.p. injections of 20 million viable BT-20 cells in complete Freund's adjuvant were administered twice at 3-wk intervals. Seven months later, 100 μg of the membrane fraction of BT-20 cells was injected intravenously. The spleen cells from two mice were used 4 days later for hybridization with SP2/O murine myeloma cells by the established polyethylene glycol hybridization method (*26*). Cloning and subcloning to establish monoclonality have been reported (*25*). Higher concentrations of 10-3D2 for in vivo imaging studies were produced in BALB/c mice primed with pristane in ascitic form. The ascitic fluids obtained were made 40% saturated with ammonium sulfate to precipitate the antibody. Then, after dialysis in PBS (0.01 *M* phosphate in 0.15 *M* NaCl, pH 7.4), the antibody fraction was further purified by protein-A immunoadsorption (*27*). 10-3D2 was determined to be IgG_1 isotype. Electrophoresis in 13% sodium dodecyl sulfate polyacrylamide gel (*28*) showed the antibody to be 95% pure, with no contaminating transferrin.

Preparation of 10-3D2 Fab and $F(ab')_2$ fragments. Fab fragments were prepared by papain digestion of whole antibody by the established method (*29*). Fab fragments were separated from Fc and undigested monoclonal antibodies by protein-A immunoadsorption, which binds Fc and whole antibodies (*27*). Fab recovered in the fall-through fractions was pooled, concentrated by vacuum dialysis to ~3–5 mg/ml, then dialyzed in 0.1 *M* $NaHCO_3$ for subsequent covalent coupling to diethylenetriaminepentaacetic acid (DTPA) (*20,21,30*).

$F(ab')_2$ fragments were prepared by pepsin digestion of whole 10-3D2 in 0.1 *N* acetate, pH 4.5, as previously reported (*31*). $F(ab')_2$ fragments were separated from undigested 10-3D2 by protein-A immunoadsorption (*27*), then further purified by Sephadex-G100 column chromatography (*32*). The $F(ab')_2$ fragments were also dialyzed against 0.1 *M* $NaHCO_3$ for covalent coupling to DTPA (*20,21,30*). Contamination of the $F(ab')_2$ and Fab preparations with intact antibody was determined by Ouchterlony's method of double diffusion in 1% agarose (*33*). Only preparations that showed lines of partial identity with whole antibody were used. Preparations showing contamination of intact antibody or Fc in Fab preparations were submitted for repurification by protein-A immunoadsorption.

DTPA coupling of 10-3D2. Whole 10-3D2, $F(ab')_2$, and Fab fragments were covalently coupled with DTPA by the carboxy/carbonic anhydride method of Krejcarek and Tucker (*30*), as previously described for small quantities of antibodies (*20,21*). The DTPA-linked proteins were dialyzed extensively in saline (6 l) overnight, then against 0.3 *M* PBS, pH 8.0. The DTPA-linked 10-3D2 monoclonal antibody and the Fab and $F(ab')_2$ fragments were stored frozen until used.

Indium-111 labeling of DTPA linked 10-3D2 (DTPA 10-3D2). We have developed a gentle method of labeling DPTA-antibodies with In-111 using sodium citrate as a transchelator at pH 5.5 to 6.0. Specifically, 8–10 mCi of indium-111 were pretreated with 200 μl of 1 *M* sodium citrate, pH 5.5, for 30 min, then added to an aliquot of 250–500 μg of either DTPA-labeled 10-3D2, Fab, or $F(ab')_2$. The final concentration of citrate was ~0.5 *M*. The mixture was stirred vigorously, then let stand at room temperature for another 30 min. Bound and free In-111 were separated by column chromatography (10-ml Sephadex-G25 column topped with 1 ml Chelex-100 and equilibrated; eluted with lactated Ringer's solution). Indium-111 bound to DTPA-linked proteins was eluted in the void volume. The peak activity was pooled, then ~200 μCi of In-111·DTPA·10-3D2 (300–500 μl per nude mouse) were used in tumor detection and visualization studies. The specific activity of In-111 used was ~10 mCi per mg of whole 10-3D2, Fab, or MOPC-21, and 16.7 mCi per mg of $F(ab')_2$.

Iodine-125 labeling of control murine myeloma IgG. Radioiodination of control murine myeloma IgG (MOPC-21) with I-125 was by the lactoperoxidase procedure of Marchalonis (*34*). Bound and free I-125 were separated by Sephadex-G25 (10 ml) chromatography. I-125 labeled normal IgG was stored frozen until used. MOPC-21 isotype IgG_1 was used to match the isotype of 10-3D2.

Tumor implantation. Solid BT-20 or HS-578T tumors were passed from nude mouse to nude mouse by sterile surgical implantation of 1 to 1.5 mm cubed pieces of the tumors. The tumor was implanted in the left shoulder or upper abdominal region through a small surgical incision at least 10 days before the mice were used in the tumor-imaging studies.

Experimental protocol of tumor imaging. Nude mice hosting either BT-20 or HS-578T human mammary tumors were used in three studies: The first compared the distribution of whole antibody 10-3D2 with that of Fab, $F(ab')_2$, MOPC-21, and transferrin; the second compared a specific antibody in two different tumors; the third showed that tumors can be visualized even if they overlie the spleen and liver or the upper abdominal region.

a). Nude mice hosting BT-20 human mammary tu-

mors were divided into four groups:

Group 1 (n = 5, 1 died at 19 hr after injection) received In-111 DTPA 10-3D2;

Group 2 (n = 8) received In-111 DTPA 10-3D2 $F(ab')_2$;

Group 3 (n = 5, 1 died after the 24-hr imaging) received In-111 DTPA 10-3D2 Fab;

Group 4 received In-111-labeled plasma (transferrin) (n = 4, 1 died at 24 hr after injection) (*35*);

Group 5 received In-111 DTPA MOPC-21.

Each mouse received 200 μCi of In-111 activity (approximately 20 μg protein) by tail-vein injection, except Group 2, which received only 167 (10 μg) μCi of In-111-labeled $F(ab')_2$ (10-3D2) per mouse.

Imaging. Each animal was immobilized with intraperitoneal 4% chloral hydrate (0.01 ml per g body weight); it was then placed prone beneath the detector. Two images were recorded with the pinhole collimator 4 cm from the back of the animal, centered over the tumor, for a period of 10 min. The camera was set to image only the upper energy peak (263 keV) of indium-111. Imaging sessions took place at 1, 24, and 48 hr following injection. After the 48-hr imaging session, the mice were killed by cervical dislocation and the biodistribution of the In-111 label was determined by scintillation well counting of the blood, heart, lungs, liver, spleen, small intestine, kidneys, and the tumors. All organs were counted whole except the blood, where an aliquot was counted and total blood volume was calculated as 8% of total body weight. All distributions were reported as % of injected dose per organ or per g of the organ. Group 1 also received simultaneously I-125-labeled myeloma IgG (10 μCi/mouse) as controls.

Data from the gamma counting of In-111 activities were corrected for physical decay and compared with a standard In-111 sample used to calibrate the efficiency of the scintillation counter. The activity in the syringe was determined in a dose calibrator before and after injection to determine the injected dose precisely.

b). In this study, two groups of six nude mice, each hosting either BT-20 or HS-578T human mammary tumors, were injected intravenously, each mouse with a mixture of 200 μCi of In-111·DTPA·10-3D2 (20 μg) and 10 μCi I-125-tagged normal IgG. Imaging was performed as above, but it was done at 1 hr after injection and at every 24 hr for the following 6 days. On Day 7 after the injection, the animals were killed and the biodistributions of both radionuclides was determined as described above. Two nude mice from each group died during the experiment. The imaging data obtained were analyzed by planimetry, to compare In-111 activity in the tumor with In-111 activity in the head region. The ratios obtained were used as figures of merit (*36*), as shown in Figs. 6 and 7.

c). A group of four mice hosting BT-20 human mammary tumors in the upper abdominal region overlying the spleen and liver were injected intravenously with 200 μCi In-111 DTPA 10-3D2 (approximately 20

TABLE 1. BIODISTRIBUTIONS OF In-111·DTPA·10-3D2 AND I-125·NIgG IN NUDE MICE (n = 4) HOSTING BT-20 HUMAN MAMMARY TUMORS, AT 48 hr AFTER I.v. INJECTION

Organ	Weight(g)*	In-111·10-3D2		I-125·IgG	
		% dose/g*	% dose/organ*	% dose/g*	% dose/organ*
Blood	1.93	7.9§	15.02	5.4	10.3
	(1.76–2.22)	(5.70–10.84)	(12.55–19.72)	(2.72–5.80)	(5.21–10.20)
Heart	0.11	3.8	0.36	1.4	0.16
	(0.10–0.13)	(2.38–4.13)	(0.30–0.43)	(1.00–1.83)	(0.10–0.23)
Lungs	0.13	5.4	0.71	2.0	0.34
	(0.10–0.16)	(4.16–6.46)	(0.63–0.90)	(1.09–3.93)	(0.19–0.53)
Liver	1.38	7.85	10.83	1.57	2.16
	(1.24–1.70)	(7.05–8.20)	(8.78–13.55)	(1.05–2.36)	(1.30–3.17)
Spleen	0.07	13.4	0.9	4.27	0.25
	(0.04–0.08)	(10.11–17.89)	(0.77–1.11)	(1.21–10.14)	(0.10–0.44)
Sm. Intest.	1.81	2.23	4.2	0.71	1.27
	(1.60–2.06)	(2.19–2.70)	(3.53–4.85)	(0.36–1.11)	(0.64–1.78)
Kidneys	0.44	10.04	4.3	1.32	0.58
	(0.38–0.53)	(7.41–11.72)	(3.85–4.98)	(0.87–2.0)	(0.33–0.83)
Tumors†	0.77	14.72‡	8.45	1.72‡	1.09
	(0.25–1.77)	(11.94–17.46)	(4.34–21.16)	(1.07–2.40)	(0.50–1.90)

* Mean, (range).

† Range of tumor size = 0.249 to 1.772g.

‡ $p < 0.001$.

§ $p > 0.05$ when compared to blood activity of In-111 DTPA MOPC-21 (Table 3).

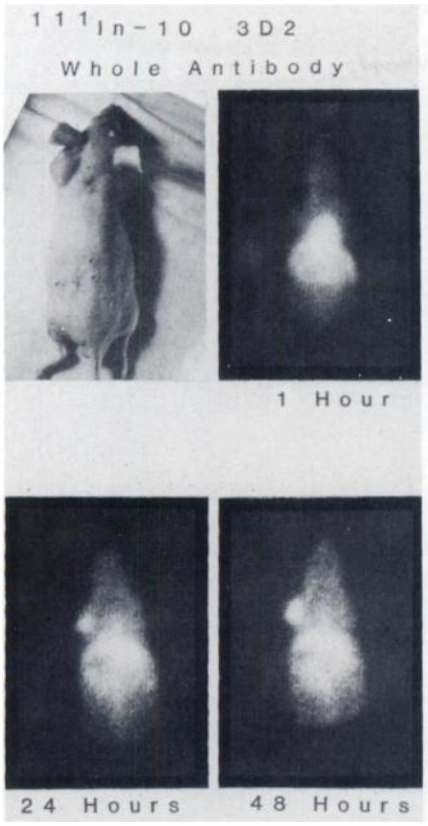

FIG. 1. Posteroanterior photograph (top left) and gamma scintigrams of nude mouse hosting 0.249-g BT-20 human mammary tumor in left shoulder region. Images obtained at 1, 24, and 48 hr after i.v. administration of In-111-labeled 10-3D2. In each image, contrast is normalized to pixel with highest count in scintigram. Tumor is distinctly visible at 24 and 48 hr, cephalad of liver and splenic activities.

μg). Imaging was performed as in Group b for 6 days. On the 7th day the animals were killed and biodistribution determined as described for Group a.

All data from scintillation counting of tissue organs were also used to calculate figures of merit (signal^2/noise, shown in the tables) using the formula:

$$\frac{\text{specific activity in tumor}}{\text{specific activity in blood}} \times \text{specific activity in tumor/g.}$$

Statistical analysis of the biodistribution data was done by applying log transformation with one-way analysis of variance, using the BMDP 1981 software from UCLA, program BMDP7D. Homogeneity of variances was checked with the Levine test.

RESULTS

At 48 hr after intravenous administration of 10-3D2, the blood activity was still high at 7.9% dose/g, but the tumors were clearly visualized, with uptakes of (14.7 ± 2.25)% dose/g (Table 1). These tumors ranged in weight from 0.2487 g to 1.7718 g in the four mice that survived to 48 hr. Even in the mouse that died at 19 hr, the tumor mass of only 0.1415 g was clearly visualized by gamma imaging.

The corresponding I-125-labeled MOPC-21 IgG controls showed only (1.72 ± 0.55)% dose/g in the tumors, and a lower blood activity than that of In-111-labeled 10-3D2. The liver distribution of In-111-labeled antibody (10.83% dose/organ) and I-125-labeled IgG control (2.16% dose/organ) were also significantly different. Figure 1 shows the corresponding posteroanterior gamma images from a representative nude mouse with BT-20 tumor, obtained at 1, 24, and 48 hr after whole-antibody injection.

Localization of the radiolabeled 10-3D2 can be appreciated as soon as 1 hr after i.v. injection in some animals. However the tumors became progressively better defined with time. When $F(ab')_2$ of 10-3D2, labeled with In-111, was used to image BT-20 in nude mice (n = 8),

TABLE 2. COMPARATIVE BIODISTRIBUTION OF In-111 DTPA 10-3D2 $F(ab')_2$ (n = 8) AND In-111 DTPA 10-3D2 Fab (n = 5) IN NUDE MICE HOSTING BT-20 HUMAN MAMMARY TUMORS, AT 48 hr AFTER i.v. ADMINISTRATION

Organ	In-111 DTPA-$F(ab')_2$ (10-3D2)			In-111 DTPA Fab (10-3D2)		
	Weight(g)*	% dose/g*	% dose/organ*	Weight(g)*	% dose/g*	% dose/organ*
Blood	1.69 ± 0.12	0.32 ± 0.07	0.53 ± 0.12	2.0 ± 0.08	0.20 ± 0.04	0.39 ± 0.09
Heart	0.11 ± 0.01	1.04 ± 0.13	0.11 ± 0.01	0.13 ± 0.01	0.37 ± 0.07	0.05 ± 0.01
Lungs	0.13 ± 0.02	1.60 ± 1.29	0.20 ± 0.15	0.16 ± 0.01	0.34 ± 0.06	0.06 ± 0.01
Liver	1.40 ± 0.22	4.55 ± 0.76	6.35 ± 0.37	1.36 ± 0.16	1.69 ± 0.33	2.25 ± 0.21
Spleen	0.10 ± 0.02	3.12 ± 0.67	0.32 ± 0.08	0.12 ± 0.02	0.93 ± 0.15	0.11 ± 0.03
Sm. Intest.	2.55 ± 0.37	0.46 ± 0.10	1.18 ± 0.29	1.60 ± 0.29	0.29 ± 0.04	0.45 ± 0.07
Kidneys	0.38 ± 0.02	40.0 ± 8.86	15.1 ± 3.06	0.45 ± 0.04	50.0 ± 13.6	22.5 ± 5.94
Tumors†	0.15 ± 0.09	5.74 ± 1.61‡	0.81 ± 0.42	0.23 ± 0.19	1.14 ± 0.23‡	0.25 ± 0.17

* Mean ± standard deviation.
† Tumor size range for $F(ab')_2$ = 0.091 to 0.365 g, for Fab = 0.1176 to 0.5729 g.
‡ $p < 0.001$.

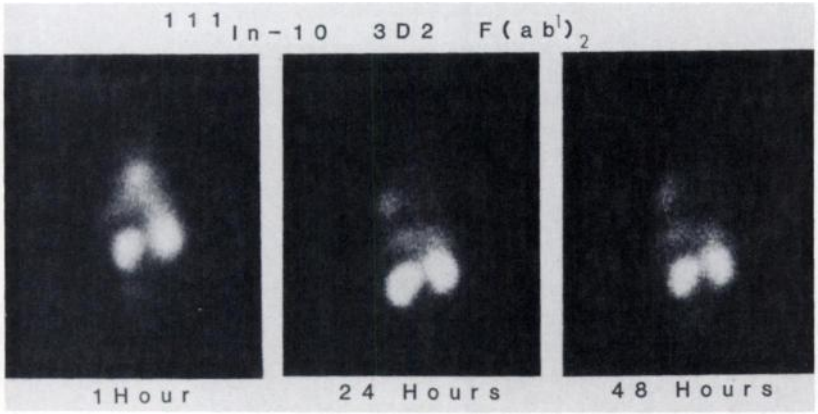

FIG. 2. Posteroanterior gamma scintigrams of nude mouse hosting BT-20 human mammary tumor (0.1004 g), obtained at 1, 24, and 48 hr after i.v. administration of In-111-labeled $F(ab')_2$ fraction of 10-3D2. Each image is normalized to pixel with highest count in field of view. One-hr image (left) showed heart, liver, spleen, and kidney activities. Tumor was distinctly visible, however, in 24- and 48-hr images, on left side, above liver and splenic activities.

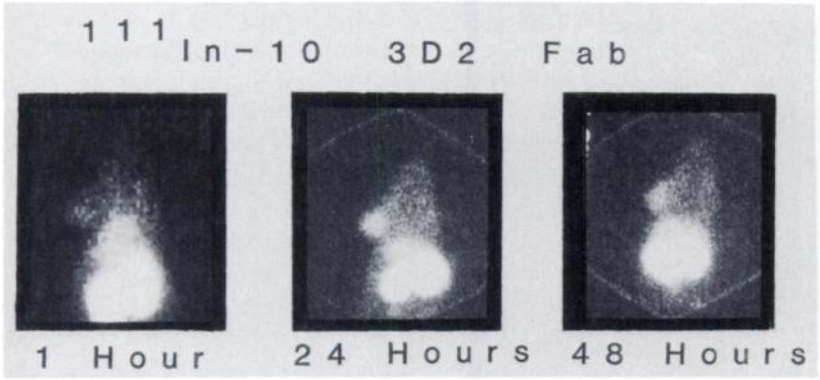

FIG. 3. Posteroanterior images of nude mouse hosting BT-20 human mammary tumor (0.1792 g), obtained at 1, 24, and 48 hr after i.v. administration of In-111-labeled 10-3D2 Fab. These images were highly contrasted in order to visualize the tumors, therefore computer display showed pixel saturation in kidneys. With this contrast enhancement, tumor can be seen clearly at 24 and 48 hr.

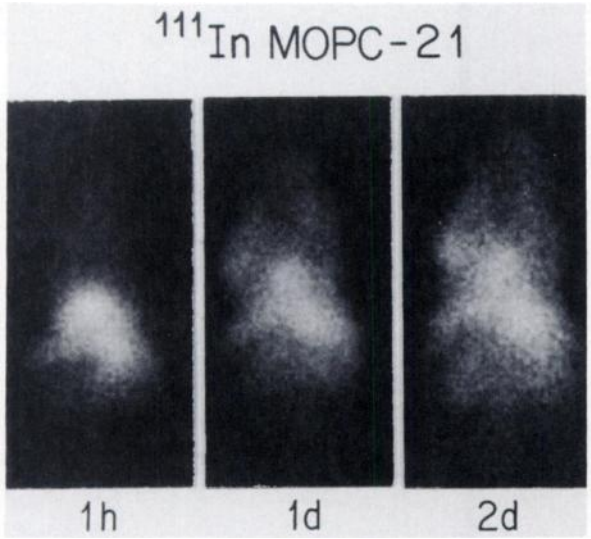

FIG. 4. Posteroanterior image of nude mouse hosting BT-20 human mammary tumor (0.1322 g), at 1, 24, and 48 hr after i.v. administration of In-111-labeled MOPC-21. In each image, contrast is normalized to hottest pixel in scintigram. There is some nonspecific uptake of In-111-labeled MOPC-21 in tumor but activity in blood is greater.

blood clearance determined at 48 hr [(0.32 ± 0.07)% dose/g] was faster than that of whole 10-3D2 [(7.9 ± 2.2)% dose/g]. Tumor uptake of $F(ab')_2$(10-3D2) at 48 hr was [(5.74 ± 1.61% dose/gm]; but the organs with the highest activity were the kidneys. The total biodistribution is shown in Table 2. The images obtained with $F(ab')_2$(10-3D2) were clearer and had less background blood activity, except for kidney activity, as shown in Fig. 2.

Fab fragments of 10-3D2 also showed specific localization in the BT-20 tumors (Table 2). Mean tumor localization was (1.14 ± 0.23)% dose/g at 48 hr after i.v. injection. Although the liver activity was low at (1.69 ± 0.33)% dose/g, the blood activity was lower at (0.2 ± 0.04)% dose/g. The highest radioactivity was observed in the kidneys [(50 ± 13.6)% dose/g]. Despite the very short residence time of Fab in the circulation, visualization of the BT-20 tumor was feasible. The high kidney activity, however, hindered visualization of the tumors (Fig. 3) and required maximal contrast enhancement for tumor display, seen as saturation of the range of the image display.

When In-111 DTPA MOPC-21 was used as a control for the imaging of BT-20 human mammary tumors in nude mice, only blood-pool activity in the tumors was observed, with no specific localization (Fig. 4). Although tumors showed (5.8 ± 1.08)% dose/g activity, the activity appears to be mainly due to the blood (Table 3), as indicated by the figure of merit (4.26) or the 0.74 ratio of tumor/blood activity (Table 4).

Table 4 shows a comparison of whole 10-3D2, its $F(ab')_2$ and Fab, and the MOPC-21 (control) distribu-

TABLE 3. BIODISTRIBUTION OF In-111-LABELED MOPC-21 IN NUDE MICE (n = 4) HOSTING BT-20 HUMAN MAMMARY TUMORS AT 48 hr AFTER I.v. ADMINISTRATION

Organ	Weight*	% dose/g*	% dose/organ*
Blood	1.83	7.86‡	14.29
	(1.58–2.08)	(6.60–8.57)	(13.55–15.37)
Heart	0.13	2.59	0.33
	(0.11–0.16)	(2.08–3.00)	(0.29–0.37)
Lung	0.16	4.02	0.62
	(0.13–0.17)	(3.66–4.41)	(0.55–0.69)
Liver	1.58	3.66	5.71
	(1.48–1.97)	(3.34–4.29)	(5.02–6.57)
Spleen	0.09	3.97	0.36
	(0.07–0.12)	(2.89–4.79)	(0.27–0.42)
Sm. Int.	1.78	1.47	2.58
	(1.42–2.29)	(1.24–1.63)	(2.12–3.11)
Kidneys	0.49	5.29	2.5
	(0.39–0.65)	(3.84–6.10)	(2.42–2.66)
Tumor	0.297	5.78†	1.80
	(0.13–0.41)	(4.33–6.96)	(0.69–2.44)

* Mean (range).
† $p < 0.001$ relative to tumor localization of 10-3D2 shown in Table 1.
‡ $p > 0.05$ compared with blood activity of In-111-DTPA-10-3D2 (Table 1).

TABLE 4. COMPARATIVE TUMOR UPTAKE OF 10-3D2 WHOLE ANTIBODY, $F(ab')_2$, AND Fab

Ab	Tumor % dose/g	(T/B)*	Figure of merit†	X/Fab‡	Liver % dose/g	Y/Fab§
IgG	14.7 ± 2.25	1.82¶	27.43	12.91	7.85 ± 0.54	4.64
$F(ab')_2$	5.74 ± 1.61	17.94¶	102.96	5.04	4.55 ± 0.76	2.69
Fab	1.14 ± 0.23	5.7¶	6.50	1.0	1.69 ± 0.33	1.0
MOPC-21	5.8 ± 1.08	0.74	4.26	NA	3.66 ± 0.44	NA

* (T/B) = Tumor specific activity/blood specific activity per gram.
† (Tumor specific activity/blood specific activity) X tumor specific activity per g.
‡ Tumor activity of whole 10-3D2 or its $F(ab')_2$/tumor activity of Fab per g.
§ Liver activity of whole 10-3D2 or its $F(ab')_2$/Fab liver activity per g.
¶ $p < 0.001$ relative to (tumor specific activity/blood specific activity) of MOPC-21.
NA: Not applicable.

tions relative to Fab localization, with each figure of merit calculated from the biodistribution data. Ratios of whole Ab:Fab in the tumor and liver are 12.9 and 4.6, and $F(ab')_2$:Fab were 5.0 and 2.7. The highest figure of merit was obtained with $F(ab')_2$ next with whole Ab at 27.43, then with Fab at 6.5, and the lowest with control MOPC-21 at 4.36.

When In-111 chloride was labeled to plasma and administered i.v. into animals with BT-20 human mammary tumors, uptake of the In-111 activity in the tumor was (3.8 ± 0.8)% dose/g. The biodistribution at 48 hr after administration is shown in Table 5. Although blood activity was only (0.83 ± 0.03)% dose/g, liver uptake [(6.67 ± 1.58)% dose/g) was very similar to that with In-111-labeled 10-3D2 [(7.85 ± 0.54)% dose/g]. However, the extravascular distribution appeared to be greater than that obtained with In-111-labeled antibody. Figure 5 shows $^{111}InCl_3$ (labeled plasma) gamma images of nude mice with BT-20 tumors at 1, 24, and 48 hr after i.v. injection of 200 μCi of In-111 activity. The definition of the tumor is poor relative to the images obtained with specific monoclonal 10-3D2 (Fig. 1).

Since the blood activity of In-111-labeled 10-3D2 remained too high at 48 hr after injection, we endeavored to image a group of six nude mice with BT-20 tumors at

TABLE 5. BIODISTRIBUTION OF In-111-LABELED MOUSE PLASMA IN NUDE MICE (n = 3) HOSTING BT-20 HUMAN MAMMARY TUMORS AT 48 hr AFTER i.v. ADMINISTRATION

Organ	In-111-labeled plasma distribution		
	Weight(g)*	% dose/g*	% dose/organ*
Blood	1.65	0.83	1.53
	(1.44–1.83)	(0.81–0.86)	(1.49–1.59)
Heart	0.12	2.34	0.27
	(0.11–0.13)	(2.12–2.64)	(0.24–0.30)
Lungs	0.15	3.64	0.54
	(0.14–0.17)	(3.22–4.27)	(0.44–0.71)
Liver	1.60	6.67	10.38
	(1.29–1.86)	(5.45–8.46)	(10.09–10.90)
Spleen	0.09	5.12	0.44
	(0.07–0.11)	(3.73–6.92)	(0.28–0.50)
Sm. Intest.	1.65	2.71	4.38
	(1.44–1.97)	(2.33–3.46)	(3.57–4.99)
Kidneys	0.42	16.65	7.67
	(0.38–0.61)	(13.21–19.79)	(6.50–8.45)
Tumor	0.53	3.80	2.06
	(0.38–0.75)	(2.89–4.44)	(1.31–3.34)

* Mean (range).

1 hr, 1, 2, 3, 4, 5, and 6 days after administration of the radiolabeled 10-3D2. Table 6 shows the biodistribution, performed on Day 7. Blood activity was reduced to (5.74 ± 0.4)% dose/g on the 7th day, whereas mean tumor activity was increased to (21.97 ± 4.44)% dose/g. Blood activity of control I-125-labeled myeloma IgG was (2.35 ± 0.40% dose/g in these same animals, and the mean tumor activity was only (1.05 ± 0.29)% dose/g. However, when distribution of In-111-labeled 10-3D2 was studied by the same protocol in another group of nude mice hosting another line of human mammary tumor (HS-578T) (Table 7), mean blood activity of In-111-labeled 10-3D2 at 7 days [(7.45 ± 4.15)% dose/g] was very similar to that of the nude mice hosting BT-20 tumors [(5.74 ± 0.4)% dose/g]. Mean tumor uptake was significantly less at (7.97 ± 2.41)% dose/g than in BT-20 tumors [(21.97 ± 4.44)% dose/g]. Distribution of In-111-labeled 10-3D2 in the other organs was very similar in the two groups of mice studied.

Representative gamma images are shown for nude mice hosting BT-20 (Fig. 6) and HS-578T (Fig. 7), obtained at 1 hr, and 1, 2, 3, 4, 5, and 6 days, together with the corresponding figures of merit. The data obtained by gamma imaging were used to determine the figure of merit for distribution of In-111-labeled 10-3D2 in mice with BT-20 and HS-578T. Figures of merit calculated from computer planimetry compared tumor activity with blood activity in the head region of the individual ani-

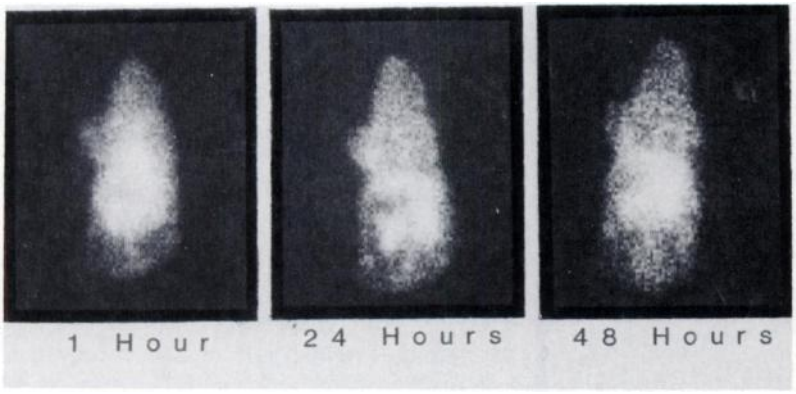

FIG. 5. Control posteroanterior images of nude mouse hosting BT-20 human mammary tumor (0.3752 g), obtained at 1, 24, and 48 hr after i.v. administration of $^{111}InCl_3$ plasma. Although outline of tumor can be observed in each image, there is no apparent specific accumulation of In-111 transferrin in tumor.

TABLE 6. BIODISTRIBUTION OF In-111 DPTA 10-3D2 AND I-125 $M_{vel}IgG$ IN NUDE MICE (n = 5) HOSTING BT-20 HUMAN MAMMARY TUMORS, AT 7 DAYS AFTER I.v. INJECTION

Organ	Weight*	In-111 DPTA 10-3D2		I-125 $M_{vel}IgG$	
		% dose/g*	% dose/organ*	% dose/g*	% dose/organ*
Blood	2.09 ± 0.23	5.74 ± 0.40	11.94 ± 0.83	2.35 ± 0.40	4.90 ± 1.05
Heart	0.15 ± 0.02	2.47 ± 0.51	0.37 ± 0.09	0.99 ± 0.31	0.15 ± 0.06
Lungs	0.18 ± 0.02	3.18 ± 0.53	0.58 ± 0.05	1.14 ± 0.34	0.21 ± 0.05
Liver	1.65 ± 0.33	6.25 ± 1.49	9.99 ± 1.05	0.77 ± 0.13	1.28 ± 0.31
Spleen	0.12 ± 0.04	8.40 ± 1.22	1.02 ± 0.22	1.38 ± 0.51	0.16 ± 0.03
Sm. Intest.	2.48 ± 0.54	1.27 ± 0.27	3.04 ± 0.40	0.38 ± 0.12	0.94 ± 0.32
Kidneys	0.50 ± 0.08	6.75 ± 2.08	3.20 ± 0.66	0.85 ± 0.23	0.41 ± 0.07
Tumor	0.83 ± 0.34	21.97 ± 4.44	17.77 ± 5.90	1.05 ± 0.29	0.92 ± 0.57

* Mean ± standard deviation.

mals. Indium-111-labeled 10-3D2 appeared to be more avid for BT-20 than for HS-578T. This has been reported also for in vitro binding studies (*25*).

Optimal localization of the radiolabeled 10-3D2 for imaging BT-20 tumors appears to occur at Day 4 after i.v. injection, whereas figures of merit indicated that optimal ratios for HS-578T occur on Day 1 or 2. When BT-20 tumors were implanted in the upper abdominal region, lying over the liver and spleen, tumors can still be visualized (Fig. 8). Tumor uptake at 7 days was (19.03 ± 8.01)% dose/g, with tumor size ranging from 0.085 to 0.404 g (0.192 ± 0.144 g).

DISCUSSION

The monoclonal antibody 10-3D2 used in this study was developed and characterized by Soule and coworkers (*25*). This antibody, raised to human mammary carcinoma cells, recognizes a 126-kd phosphoglycoprotein (pgp) associated with cells of a variety of human carcinomas. It does not bind normal mammary epithelium, a variety of control cell lines, or homogenates of normal human tissues. However, it had low but significant cross-reactivity with certain other neoplastic cell lines, including melanoma M-14, choriocarcinoma JAL-C2, lung carcinomas COLO-338 and A-549, and colon carcinoma COLO-463. It appears that 10-3D2 recognizes a tumor-associated antigen that frequently appears in mammary carcinoma; recent immunohistochemical studies have demonstrated reactivity with virtually all cells of all of 43 carcinomas of the breast, including different histologic types (Bacchi et al., unpublished). The target antigen is not specific for malig-

TABLE 7. BIODISTRIBUTION OF In-111-DPTA-10-3D2 IN NUDE MICE (n = 4) HOSTING HS-578T HUMAN MAMMARY TUMORS, AT 7 DAYS AFTER I.v. INJECTION

Organ	Wt (g)*	In-111-M-Ab-10-3D2	
		% dose/g*	% dose/organ*
Blood	1.76	7.45	12.62
	(1.52–1.92)	(2.42–12.54)	(4.66–19.06)
Heart	0.12	2.86	0.34
	(0.11–0.15)	(1.81–3.72)	(0.26–0.47)
Lungs	0.16	4.35	0.68
	(0.12–0.20)	(2.66–5.92)	(0.54–0.78)
Liver	1.53	8.74	12.54
	(1.41–1.64)	(8.10–9.23)	(10.01–13.83)
Spleen	0.14	11.08	1.45
	(0.09–0.25)	(8.77–14.81)	(0.85–2.21)
Sm. Intest.	1.93	1.90	3.58
	(1.41–2.28)	(1.54–2.74)	(2.93–4.04)
Kidneys	0.95	7.47	3.33
	(0.42–0.50)	(5.28–9.51)	(2.24–4.12)
Tumor	0.39	7.97	3.54
	(0.19–0.72)	(5.74–11.39)	(1.11–8.24)

* Mean (range).

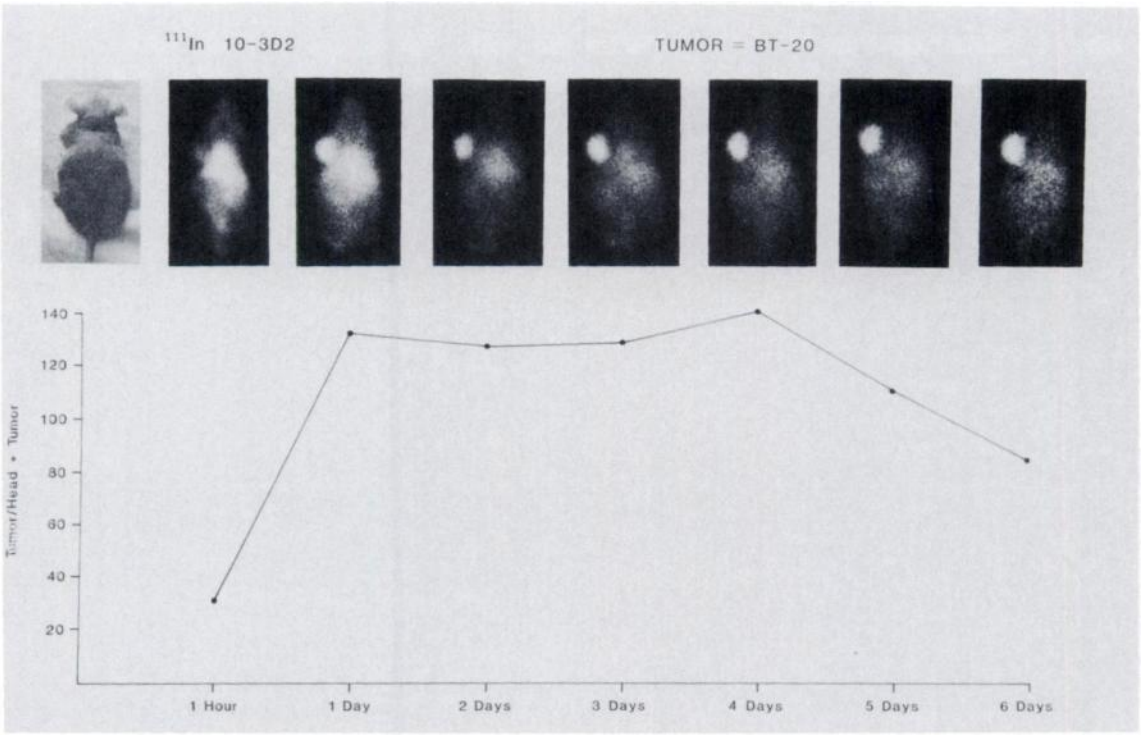

FIG. 6. Photograph (upper left) and posterior scintigrams of representative nude mouse hosting BT-20 human mammary tumor, obtained at 1 hr, and 1, 2, 3, 4, 5, and 6 days after i.v. administration of In-111-labeled 10-3D2. For each image, figure of merit (see text for explanation) is plotted below. Highest figure of merit was obtained at Day 4 and this is confirmed by highest-quality image obtained at Day 4.

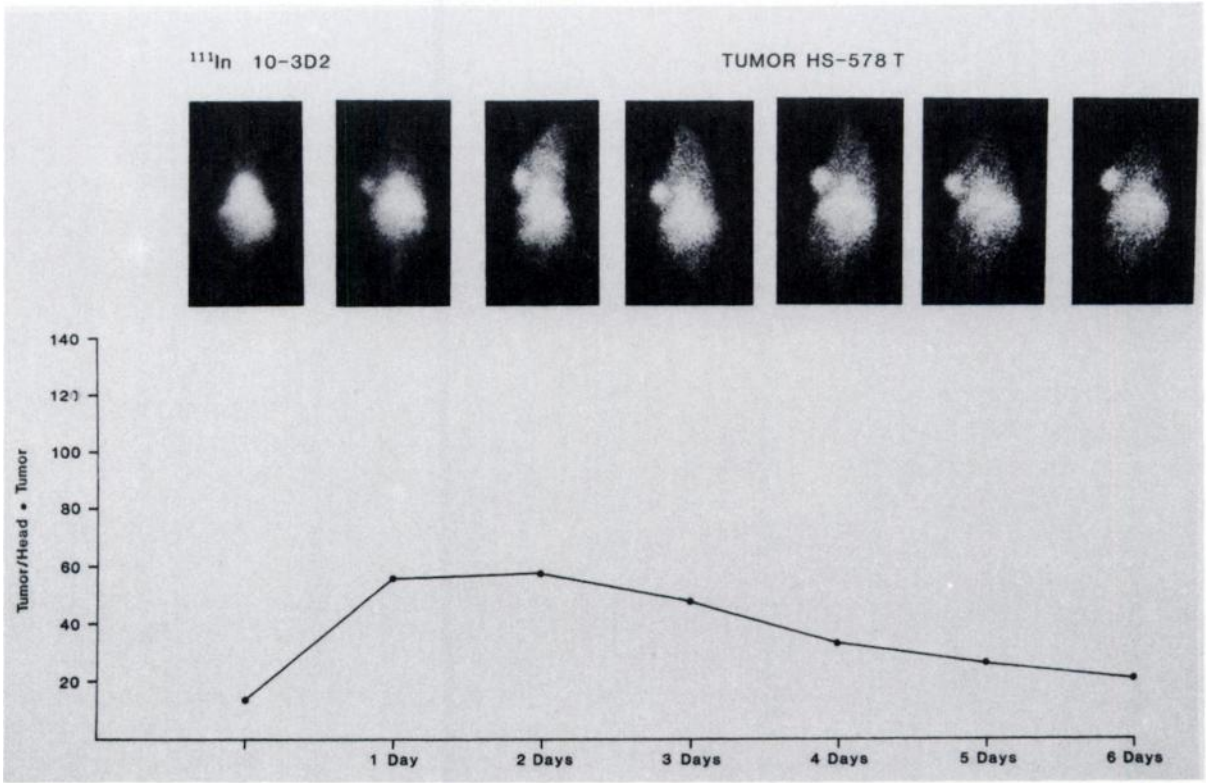

FIG. 7. Posteroanterior images of representative nude mouse hosting HS-578T human mammary tumor, obtained at 1 hr, and 1, 2, 3, 4, 5, and 6 days after i.v. administration of In-111-labeled 10-3D2. Corresponding figures of merit are plotted below. Highest figure of merit was obtained between Days 1 and 2.

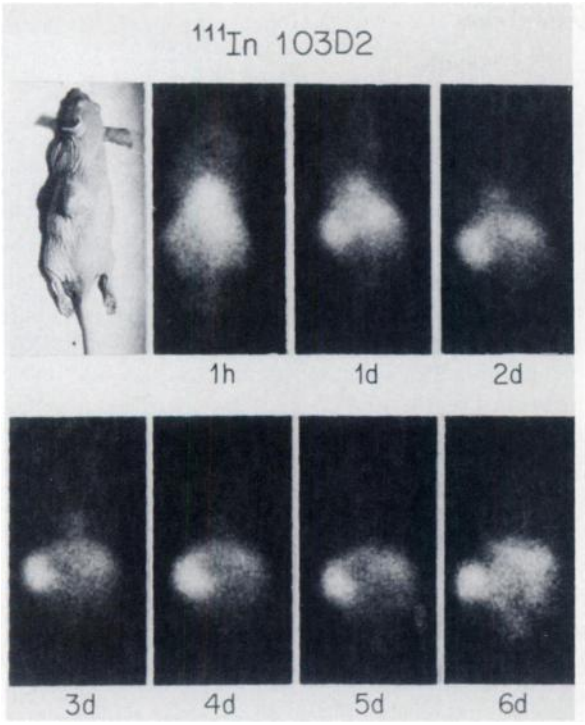

FIG. 8. Posteroanterior images of representative nude mouse hosting BT-20 human mammary tumor (0.1268 g) in upper abdominal region (top left panel), obtained at 1 hr, and 1, 2, 3, 4, 5, and 6 days after i.v. administration of In-111-labeled 10-3D2. Tumor can be seen clearly even by Day 1, despite its location over spleen and liver.

nant cells, since the benign neoplastic epithelium of fibroadenomas of the breast was also positive, but the expression of the 126-kd pgp on proliferating benign mammary epithelium should not preclude effective application.

The antibodies were labeled with In-111 by a technique initially developed for labeling antimyosin Fab to locate and visualize experimental myocardial infarctions. However, this method of labeling Fab(10-3D2) with In-111 at acidic pH could cause denaturation of the Fab. Therefore, a modified method uses indium chloride in a solution of a weak chelator, such as citrate buffers at pH 5.5. The labeling of DTPA-antibodies in 0.3*M* phosphate buffer, pH 8.0, was achieved by simple addition of this solution to the In-111 citrate solution. Transchelation of In-111, from a weak chelate such as citrate, to a strong chelate such as DTPA, was readily achieved. An average specific activity of 10 mCi/mg DTPA-antibody is usually achieved by this labeling procedure. The mild condition of labeling does not denature antibodies and their fragments. This is evident by the low in vivo liver uptake of In-111-labeled antibodies, which for intact 10-3D2 was (7.85 ± 0.54)% dose/g; for $F(ab')_2$ (4.55 ± 0.76)% dose/g; and for Fab fragments (1.69 ± 0.33)% dose/g, at 48 hr after i.v. administration (Tables 1 and 2). Recently, Scheinberg and co-workers (*22*) used an In-111-labeled monoclonal antibody-DTPA complex to image murine erythroleukemic spleen. Similarly, Hnatowich and co-workers (*23*) imaged human colorectal xenograft in nude mice. Both groups observed the mildness of the labeling procedure.

The image quality obtained with In-111-labeled 10-3D2 for visualization of BT-20 hosted in nude mice permitted tumor detection as early as 24 hr after i.v. administration of the radiolabeled monoclonal antibody (Fig. 6). In some animals, distinct uptake of In-111 activity in the tumors can be seen as early as 1-2 hr after i.v. administration of the antibody. Whether this represented visualization of only blood-pool activity is not known. The tumors were readily visible even when they lay over the spleen and liver (Fig. 8). The calculations of figure of merit demonstrate that the best target-to-background (blood activity) ratios for image visualization were obtained between 2 and 4 days when intact 10-3D2 labeled with In-111 was used to image BT-20 human mammary tumor. However, when In-111-labeled 10-3D2 was used for visualization of HS-578T, the best target-to-background ratios were obtained between 1 and 2 days after i.v. injection (Fig. 7). Comparison of the figures of merit by calculation from biodistribution data between intact 10-3D2 and its $F(ab')_2$ and Fab fragments, at 48 hr after i.v. injection (Table 4), showed that the normalized target-to-background ratios were 27.43, 102.96, and 6.5, respectively. This indicated that $F(ab')_2$ fragments of 10-3D2 are best suited for tumor detection and display by gamma imaging at 48 hr after antibody administration; intact 10-3D2 was next, while Fab was poor (Fig. 3). The corresponding figure of merit for nonspecific MOPC-21 myeloma IgG_1 was the lowest, at 4.23. This is reflected in the poor images obtained (Fig. 4).

One major obstacle not evident in the calculations of figure of merit of $F(ab')_2$ for visualization of tumors is the high radioactivity in the kidneys [(39.96 ± 8.86)% dose/g]. This is probably due to active filtration of the $F(ab')_2$ by renal clearance. It can mask detection and visualization of tumor masses in the vicinity of the kidneys. By waiting longer than 48 hr and using a radiolabel of sufficiently long half-life such as In-111 (2.7 days), it may be possible to visualize tumors close to the kidneys after the kidneys have excreted most of the $F(ab')_2$ fragments. If time is no obstacle, whole antibody appears to be best for tumor imaging, since there is progressive accumulation of radiolabeled antibody in the tumors (14.72% dose/g at 48 hr rises to 21.97% dose/g at 7 days), liver activity is minimal, and no other organs are visible by gamma imaging. Fab, however, is cleared from the circulation too quickly for appreciable tumor detection. Despite this low uptake, gamma imaging of the mammary tumors with In-111-labeled 10-3D2 Fab is still feasible.

Wilbanks and co-workers (*37*) used iodine-131-la-

beled Fab of antibodies specific to murine mammary epithelial antigen (MME) to image murine mammary tumors, and obtained (0.87 ± 0.26)% dose/g of the antibody in the tumor at 24 hr after injection. The total blood activity was only 1% of the injected dose. When intact anti-MME was used, (2.54 ± 0.23)% dose/g was observed. Although their and our data are similar, uptakes obtained in our study at 48 hr after injection of Fab and intact monoclonal 10-3D2 are greater (1.14 ± 0.23% dose/g and 14.72 ± 2.25% dose/g respectively). Tumor uptake of intact 10-3D2 was 8.6 times greater than nonspecific adsorption or blood-pool activity of radioiodine-labeled control myeloma IgG, whereas Wilbanks et al. (*37*) obtained specific uptake only 1–8 times the nonspecific. More recently, Wahl and co-workers (*24*) observed that iodine-131-labeled $F(ab')_2$ of monoclonal anti-CEA was better than intact antibody or Fab, giving more rapid specific tumor detection. The present study showed, however, that although $F(ab')_2$ of 10-3D2 had the highest normalized ratios of tumor activity to blood activity (Table 4), the gamma images demonstrated that intact 10-3D2 provided the best images of human mammary tumors hosted in nude mice (Fig. 6).

The above observations should be valid for tumor imaging with antibodies specific for tumor-associated antigens that are not secreted or released into the circulation. It is unlikely that 126-kd pgp identified by hybridoma antibody 10-3D2 is shed and interacts with the labeled antibody at sites remote from the tumor. When BT-20 or AY-726 breast-carcinoma cells were intrinsically labeled in culture with S-35 methionine, and the medium was subjected to immunoprecipitation with 10-3D2 antibody, no antigen could be demonstrated, although 126-kd pgp was clearly demonstrable in detergent lysates of the cell (*25*). The apparent shedding of the cellular antigen in vitro under conditions where detection is readily analyzed suggests that this is not a secretory protein, and interaction with antibody in the plasma should not be a significant issue. Tumors producing oncofetal proteins that are released into the circulation, such as CEA (*16*), alpha-fetoprotein (*14*), and other tumor-associated antigens (*8*,*38*) may demonstrate a different figure of merit, since circulating tumor-associated antigens could interfere with the normal circulation and clearance of the administered antibodies. Whether intact antibody, $F(ab')_2$, or Fab is most effective for the imaging of tumors that secrete tumor-associated antigens into the circulation must be determined individually. Our study also demonstrated that different human mammary-tumor lines, with different in vitro binding capacity by 10-3D2 (*25*), showed different in vivo localization and quality of tumor images. The BT-20 human mammary-tumor line showed the highest in vitro binding of 10-3D2, and also had very high in vivo localization of the In-111-labeled 10-3D2: (21.97 ± 4.4)% dose/g at 7 days after i.v. injection. HS-578T, which had lower in vitro 10-3D2 binding (*25*), also had low in vivo localization of 10-3D2 [(7.97 ± 2.41)% dose/g] at 7 days. The figure of merit (Fig. 6) shows that normalized best uptake-to-background activity of 10-3D2 for BT-20 occurred between 2 and 4 days, and for HS-578T, between 1 and 2 days (Fig. 7). This indicated that with BT-20 tumors there was continuous concentration of radiolabeled 10-3D2 until 4 days, whereas HS-578T tumors showed possible saturation of binding by radiolabeled 10-3D2 as early as 1 to 2 days.

Thus, this study demonstrated that the labeling of antibody, $F(ab')_2$, or Fab with In-111 through the use of a bifunctional chelator, DTPA, is a very gentle process that causes no apparent denaturation. Indium-111-labeled monoclonal antibody 10-3D2, specific for a 126-kd pgp tumor-associated antigen, can be used to visualize tumors hosted in nude mice by gamma scintigraphy. At least in this model, where no circulating tumor-associated antigen is detectable, $F(ab')_2$ fragments of 10-3D2 provided better target-to-background ratios for gamma imaging at 48 hr after i.v. administration, compared with intact 10-3D2 or its Fab fragments. And finally, human mammary tumors with possible differential concentration of the tumor-associated antigen 126-kd pgp showed different rates of uptake and saturation with monoclonal antibody 10-3D2.

ACKNOWLEDGMENT

This work was supported by Grant CH-28166 from the National Cancer Institute.

REFERENCES

1. EHRLICH P, HERTA CA, SHIGA K: Ueber emige Verwendungen der Naphtochinonsulfosaure. *Z Physiol Chem* 61: 379–392, 1904
2. PRESSMAN D, KEIGHLEY G: The zone of activity of antibodies as determined by the use of radioactive tracers; the zone of activity of nephrotoxic antikidney serum. *J Immunol* 59: 141–146, 1948
3. BALE WF, SPAR IL, GOODLAND R: In vivo purification of I^{131} labeled localizing antirat lymphosarcoma antibody. *J Immunol* 80:482–494, 1958
4. PRESSMAN D: The development and use of radiolabeled antitumor antibodies. *Cancer Res* 40:2960–2964, 1980
5. DAY ED, PLANINSEK JA, PRESSMAN D: Localization of radioiodinated antibodies in rats bearing tumors induced by N-2-fluorenylacetamide. *J Natl Cancer Inst* 25:787–802, 1960
6. DAY ED, PLANINSEK JA, PRESSMAN D: Specific localization in vivo of anti-hepatoma antibodies in autochthonous rat hepatomas. *J Natl Cancer Inst* 27:1107–1114, 1961
7. GOLDENBERG DM, KIM EE, DELAND FH, et al: Clinical radioimmunodetection of cancer with radioactive antibodies to human chorionic gonadotropin. *Science* 208:1284–1286, 1980
8. QUINONES J, MIZEJEWSKI G, BEIERWALTES WH: Choriocarcinoma scanning using radiolabeled antibody to chorionic gonadotropin. *J Nucl Med* 12:69–75, 1971

9. MACH JP, CARREL S, FORNI M, et al: Tumor localization of radiolabeled antibodies against carcinoembryonic antigen in patients with carcinoma. *N Engl J Med* 303:5-10, 1980
10. SPAR IL, BALE WF, MARRACK D, et al: 131-I-labeled antibodies to human fibrinogen. Diagnostic studies and therapeutic trials. *Cancer* 20:865-870, 1967
11. GOLDENBERG DM, PRESTON DF, PRIMUS J, et al: Photoscan localization of GW-39 tumors in hamsters using radiolabeled anticarcinoembryonic antigen immunoglobulin G. *Cancer Res* 34:1-9, 1974
12. BELITSKY P, GHOSE T, AQUINO J, et al: Radionuclide imaging of primary renal-cell carcinoma by I-131-labeled antitumor antibody. *J Nucl Med* 19:427-430, 1978
13. SPAR IL, GOODLAND RL, BALE WF: Localization of ^{131}I labeled antibody to rat fibrin in transplantable rat lymphosarcoma. *Proc Soc Exp Biol Med* 100:259-262, 1959
14. KIM EE, DELAND FH, NELSON MO, et al: Radioimmunodetection of cancer with radiolabeled antibodies to α-fetoprotein. *Cancer Res* 40:3008-3012, 1980
15. LANG PH, MCINTIRE KR, WALDMANN TA, et al: Serum alpha fetoprotein and human chorionic gonadotropin in the diagnosis and management of nonseminomatous germ-cell testicular cancer. *N Eng J Med* 295:1237-1240, 1976
16. GOLDENBERG DM, DELAND F, KIM E, et al: Use of radiolabeled antibodies to carcinoembryonic antigen for the detection and localization of diverse cancers by external photoscanning. *N Engl J Med* 298:1384-1388, 1978
17. KOHLER G, MILSTEIN C: Continuous cultures of fused cells secreting antibody of predefined specificity. *Nature* (London) 256:495-497, 1975
18. BALLOU B, LEVINE G, HAKALA T, et al: Tumor location detected with radioactivity labeled monoclonal antibody and external scintigraphy. *Science* 206:844-847, 1979
19. MACH JP, BUCHEGGER F, FORNI M, et al: Use of radiolabeled monoclonal anti-CEA antibodies for the detection of human carcinoma by external photoscanning and tomoscintigraphy. *Immunol Today* 2:239-249, 1981
20. KHAW BA, FALLON JT, STRAUSS HW, et al: Myocardial infarct imaging of antibodies to canine cardiac myosin with indium-111-diethylenetriamine pentaacetic acid. *Science* 209:295-297, 1980
21. KHAW BA, STRAUSS HW, CARVALHO A, et al: Technetium-99m labeling of antibodies to cardiac myosin Fab and to human fibrinogen. *J Nucl Med* 23:1011-1019, 1982
22. SCHEINBERG DA, STRAND M, GANSOW OA: Tumor imaging with radioactive metal chelates conjugated to monoclonal antibodies. *Science* 215:1511-1513, 1982
23. HNATAWICH DJ, LAYNE WW, CHILDS RL, et al: Radioactive labeling of antibody: A simple and efficient method. *Science* 220:613-615, 1983
24. WAHL RL, PARKER CW, PHILPOTT GW: Improved radioimaging and tumor localization with monoclonal F(ab')2. *J Nucl Med* 24:316-325, 1983
25. SOULE HR, LINDER E, EDGINGTON TS: Membrane 126-kilodalton phosphoglycoprotein associated with human carcinomas identified by a hybridoma antibody to mammary carcinoma cells. *PNAS* 80:1332-1336, 1983
26. GEFTER ML, MARGUILIES DH, SCHARFF MD:A simple method for polyethylene glycol-promoted hybridization of mouse myeloma cells. *Somatic Cell Genet* 3:231-236, 1977
27. EY PL, PROWSE SJ, JENKINS CR: Isolation of pure IgG, IgG_{2a} and IgG_{2b} immunoglobulins from mouse serum using protein A-sepharose. *Immunochem* 15:429-436, 1978
28. LAEMMLI UK: Cleavage of structural proteins during the assembly of the head of bacteriophage T_4. *Nature* 227: 680-685, 1970
29. PORTER RR: The hydrolysis of rabbit κ-globulin and antibodies with crystalline papain. *Biochem J* 73:119-126, 1959
30. KREJCAREK GE, TUCKER KL: Covalent attachment of chelating groups to macromolecules. *Biochem Biophys Res Comm* 77:581-585, 1977
31. EDLEMAN GM, MARCHALONIS JJ: Methods used in studies of the structure of immunoglobulins. In *Methods in Immunology and Immunochemistry*. Vol I, Williams CA, Chase MW, eds. New York, Academic Press, 1967, pp 422-423
32. KHAW BA, BELLER GA, HABER E, et al: Localization of cardiac myosin-specific antibody in myocardial infarction. *J Clin Invest* 58:439-446, 1976
33. OUCHTELONY O: Antigen-antibody reactions in gels. *Acta Pathol Microbiol Scand* 32:231-240, 1953
34. MARCHALONIS JJ: An enzymatic method for the trace iodination of immunoglobulins and other proteins. *Biochem J* 113:299-305, 1969
35. CASTRONOVO FP JR, WAGNER HN JR: Comparative toxicity and pharmacodynamics of ionic indium chloride and hydrated indium oxide. *J Nucl Med* 14:677-682, 1973
36. WAGNER HN JR, EMMONS H: Characteristics of an ideal radiopharmaceutical. In *Radioactive Pharmaceuticals*. U.S. Atomic Energy Commission—Division of Technical Information. Andrews GA, Kniseley RM, Wagner HN Jr., eds. 1966, pp 1-32
37. WILBANKS T, PETERSON JA, MILLER S, et al: Localization of mammary tumors in vivo with ^{131}I-labeled Fab fragments of antibodies against mouse mammary epithelial(MME) antigens. *Cancer* 48:1768-1775, 1981
38. ESHHAR Z, ORDER SE, KATZ DH: Ferritin, a Hodgkin's disease associated antigen. *Proc Natl Acad Sci* 71:3956-3960, 1974